

A NON-ELEMENT METHOD OF SOLVING THE TWO-DIMENSIONAL NAVIER-LAMÉ EQUATION IN PROBLEMS WITH NON-HOMOGENEOUS POLYGONAL SUBREGIONS

EUGENIUSZ ZIENIUK AND AGNIESZKA BOŁTUĆ

*University of Białystok, Institute of Computer Science,
Sosnowa 64, 15-887 Białystok, Poland
{ezienuk, aboltuc}@ii.uwb.edu.pl*

(Received 5 November 2007)

Abstract: The paper introduces a parametric integral equation system (PIES) for solving 2D boundary problems defined on connected polygonal domains described by the Navier-Lame equation. Parametric linear functions were applied in the PIES to define analytically the polygonal subregions' interfaces. Only corner points and additional extreme points on the interface between the connected subregions are posed to practically define a polygonal domain. An important advantage of this approach is that the number of such points is independent of the area of identically shaped domains due to the elimination of traditional elements from modeling, the number of those elements being dependent on the domain's surface area. In order to test the reliability and effectiveness of the proposed method, test examples are included in which areas of displacements and stresses are analyzed in each subregion.

Keywords: Navier-Lamé equation, boundary problems, subregions, PIES

1. Introduction

The main problem in solving multi-dimensional boundary problems is accounting for domains of varying shapes. The most popular methods for solving boundary problems described by the Navier-Lamé equation are FEM and BEM [1, 2]. The development of these methods, particularly of the BEM method, is described in detail in [3–6]. The discretization used in FEM enables including different domains and applying various material constants to each element. Lastly, this approach involves preparation of large amounts of input data necessary for modeling boundary problems. In order to avoid the problems connected with traditional elements, it is necessary to elaborate a method that would not require traditional finite or boundary elements. This is possible by means of curves, used in computer graphics [7] and applied to describe the boundary geometry of boundary integral equations (BIE).

As a result of analytically combining curves with BIEs, an original parametric integral equation system (PIES) [8–10] has been obtained. Bézier [9] and Hermite [10] curves are used to describe smoothly the boundary geometry. They are very effective, as they enable continuous creation of any domains by means of a small number of Bézier or de-Boor control points. The definition of a polygonal domain requires only corner points to be set [8].

The PIES's numerical solution is reduced to approximating the boundary functions using known numerical methods. As a result of approximating the PIES by means of the pseudospectral method [11], an approximate system of algebraic equations is obtained. The number of equations in such systems is much less than in the FEM or even the BEM methods. The results obtained for examples solved earlier are more accurate than those obtained from other, traditional-element methods. Considering the method's advantages, it will be interesting to perform further research on problems with wider applications.

In this paper, a non-element method is proposed for solving boundary problems described on connected polygonal subregions with differing material constants. For a practical definition of two-dimensional polygonal domains only their corner points have been set; in order to band subregions, some compatibility conditions have been imposed at common boundary. Solutions obtained from a large number of test examples have confirmed high effectiveness and accuracy of the proposed method.

2. Traditional and proposed definitions of subregions

Two methods are applied to solve boundary problems defined by the Navier-Lamé equation: the finite element method (FEM) and the boundary element method (BEM) [1, 2]. Traditional FEM (see Figure 1a) is characterized by discretization of the whole domain into finite elements and is thus technically the most readily applicable to problems with subregions Ω_t of different material constants E_t, ν_t ($t = 1, 2, \dots, m$), where m is the number of subregions. As shown in Figure 1a, setting different material constants below and above the common interface I , automatically enables consideration of subregions Ω_t ($t = 1, 2$). The method's disadvantage is the necessity to use large numbers of nodes and thus solving of complex systems of algebraic equations.

From the point of view of the amount of required input data, the BEM method is more effective, because only boundary discretization is required (see Figure 1b) and thus less input data (nodes) are required than in the FEM method. Compatibility conditions on common interfaces I between the connected subregions [2] must be fulfilled when applying the method to problems defined on domains Ω built of subregions Ω_t ($t = 1, 2$).

The domain shown in Figures 1a and 1b could be defined more effectively than in BEM by setting a less input data. Actually, it could be defined merely with corner points P_i ($i = 0, 1, 2, 3, 4, 5$) of the polygonal domain (*cf.* Figure 1c). An important advantage of such modeling is that the number of corner points used is independent of the area of domains Ω of the same shapes. In other words, it is not necessary

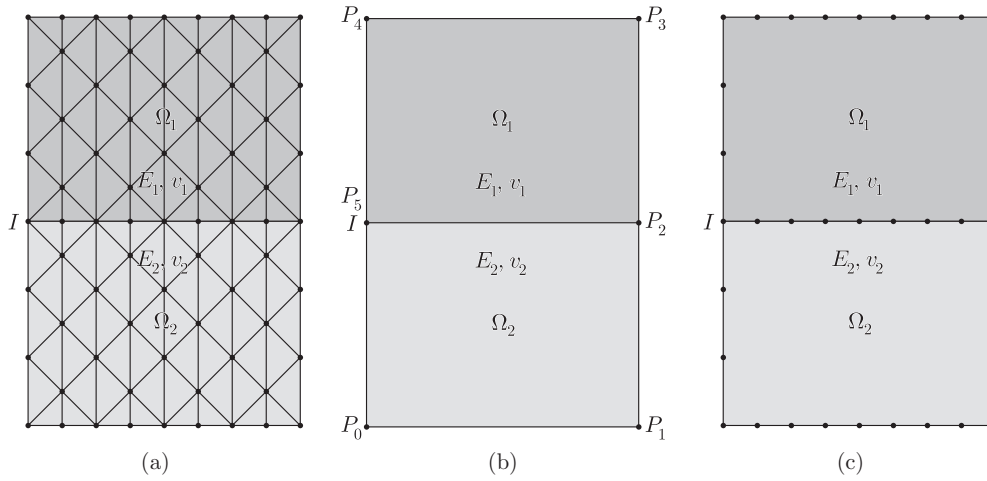


Figure 1. Traditional and proposed definitions of connected regions $\Omega = \Omega_1 + \Omega_2$: (a) traditional finite elements, (b) traditional boundary elements, (c) proposed corner points

(unlike FEM and BEM) to introduce more input data when increasing the domain area. A modification of the traditional boundary integral equation (BIE) was required in order to apply this approach to boundary problems, as follows [2]:

$$\frac{1}{2} \mathbf{u}(\mathbf{x}) = \int_{\Gamma} \mathbf{U}^*(\mathbf{x}, \mathbf{y}) \mathbf{p}(\mathbf{y}) d\Gamma(\mathbf{y}) - \int_{\Gamma} \mathbf{P}^*(\mathbf{x}, \mathbf{y}) \mathbf{u}(\mathbf{y}) d\Gamma(\mathbf{y}) + \int_{\Omega} \mathbf{U}^*(\mathbf{x}, \mathbf{y}) \mathbf{b}(\mathbf{y}) d\Omega(\mathbf{y}), \quad (1)$$

where $\mathbf{p}(\mathbf{y}) \equiv \frac{\partial \mathbf{u}(\mathbf{y})}{\partial \mathbf{n}(\mathbf{y})}$ and $\mathbf{P}^*(\mathbf{x}, \mathbf{y}) \equiv \frac{\partial \mathbf{U}^*(\mathbf{x}, \mathbf{y})}{\partial \mathbf{n}(\mathbf{y})}$, $\mathbf{x}, \mathbf{y} \in \Gamma$.

In Equation (1), boundary geometry is defined generally by means of a boundary integral; therefore, physical consideration of the boundary is possible only after its division into boundary elements. Application of the proposed modeling approach requires a modification of the traditional BIE such that boundary geometry could be defined by means of corner points. The modification was performed for homogeneous domains and Laplace's equation in paper [8], where the modified BIE was called a parametric integral equation system (PIES) [9, 10].

2.1. Parametric integral equation system (PIES) for Navier-Lamé equations

Parametric integral equation systems (PIES) can be used to solve Navier-Lamé equations with any boundary conditions and polygonal domains Ω_t . Obtaining a PIES for a homogenous polygonal region and Laplace's equation was presented in paper [12], in [9] for domains modeled by Bézier curves. A PIES for the Navier-Lamé equation was obtained in a way similar to the Laplace equation case, as presented in papers [9, 12]. The PIES for a Navier-Lamé equation with polygonal domains has the following form [13]:

$$\frac{1}{2} \mathbf{u}_p(s_1) = \sum_{r=1}^n \mathbf{J}_r \int_{s_{r-1}}^{s_r} \{ \bar{\mathbf{U}}_{pr}^*(s_1, s) \mathbf{p}_r(s) - \bar{\mathbf{P}}_{pr}^*(s_1, s) \mathbf{u}_r(s) \} ds, \quad (2)$$

$$s_{p-1} \leq s_1 \leq s_p, \quad s_{r-1} \leq s \leq s_r.$$

Integrand functions $\bar{U}_{pr}^*(s_1, s)$ and $\bar{P}_{pr}^*(s_1, s)$ of Equation (2) are the PIES's kernels and have the following form:

$$\bar{U}_{pr}^*(s_1, s) = -\frac{1}{8\pi(1-\nu)\mu} \begin{bmatrix} (3-4\nu)\ln(\eta) - \frac{\eta_1^2}{\eta^2} & -\frac{\eta_1\eta_2}{\eta^2} \\ -\frac{\eta_1\eta_2}{\eta^2} & (3-4\nu)\ln(\eta) - \frac{\eta_2^2}{\eta^2} \end{bmatrix}, \quad (3)$$

where $\eta = [\eta_1^2 + \eta_2^2]^{1/2}$, $\eta_1 = \Gamma_r^{(1)}(s) - \Gamma_p^{(1)}(s_1)$, $\eta_2 = \Gamma_r^{(2)}(s) - \Gamma_p^{(2)}(s_1)$ and $\Gamma_k^{(i)}(s)$, $i = 1, 2$, $k = r, p$ are linear parametric functions. Only the polygon's cornerpoints are posed for its definition.

The second integrand function of Equation (2) is given in the form of the following matrix:

$$\bar{P}_{pr}^*(s_1, s) = -\frac{1}{4\pi(1-\nu)\eta} \begin{bmatrix} P_{11} & P_{12} \\ P_{21} & P_{22} \end{bmatrix}, \quad p, r = 1, 2, \dots, n, \quad (4)$$

where

$$\begin{aligned} P_{11} &= \left\{ (1-2\nu) + 2\frac{\eta_1^2}{\eta^2} \right\} \frac{\partial\eta}{\partial\mathbf{n}}, & P_{12} &= \left\{ 2\frac{\eta_1\eta_2}{\eta^2} \frac{\partial\eta}{\partial\mathbf{n}} - (1-2\nu) \left[\frac{\eta_1}{\eta}n_2 + \frac{\eta_2}{\eta}n_1 \right] \right\}, \\ P_{21} &= \left\{ 2\frac{\eta_2\eta_1}{\eta^2} \frac{\partial\eta}{\partial\mathbf{n}} - (1-2\nu) \left[\frac{\eta_2}{\eta}n_1 + \frac{\eta_1}{\eta}n_2 \right] \right\}, & P_{22} &= \left\{ (1-2\nu) + 2\frac{\eta_2^2}{\eta^2} \right\} \frac{\partial\eta}{\partial\mathbf{n}}, \\ & & \frac{\partial\eta}{\partial\mathbf{n}} &= \frac{\partial\eta_1}{\partial\eta}n_1 + \frac{\partial\eta_2}{\partial\eta}n_2. \end{aligned}$$

whilst ν, μ are material constants in the Ω_t domain, and $n_1^{(j)}$ and $n_2^{(j)}$ are the components of a unit vector normal to the r segments.

Unlike the traditional BIE, the PIES is not defined on the boundary but on the straight line in the parametric reference system, for any boundary geometry. The boundary geometry is analytically defined in kernels (3) and (4) by means of parametric linear functions. In practice, only corner points of the polygon are set to define it, following which the PIES boundary geometry is created automatically. Modification of the corner points' coordinates brings about automatic modification of the whole considered geometry.

3. Solution in the domain for displacements

Having a solution for the boundary, we can obtain one for the Ω_t domain for displacements by means of the following integral identity [13]:

$$\mathbf{u}(\mathbf{x}) = \sum_{r=1}^n \mathbf{J}_r \int_{s_{r-1}}^{s_r} \left\{ \hat{U}_r^*(\mathbf{x}, s) \mathbf{p}_r(s) - \hat{P}_r^*(\mathbf{x}, s) \mathbf{u}_r(s) \right\} ds, \quad s_{r-1} \leq s \leq s_r. \quad (5)$$

The first integrand function of Equation (5) is presented as the following matrix:

$$\hat{U}_r^*(\mathbf{x}, s) = -\frac{1}{8\pi(1-\nu)\mu} \begin{bmatrix} (3-4\nu)\ln(\tilde{r}) - \frac{\tilde{r}_1^2}{\tilde{r}^2} & -\frac{\tilde{r}_1\tilde{r}_2}{\tilde{r}^2} \\ -\frac{\tilde{r}_1\tilde{r}_2}{\tilde{r}^2} & (3-4\nu)\ln(\tilde{r}) - \frac{\tilde{r}_2^2}{\tilde{r}^2} \end{bmatrix}, \quad (6)$$

where $\tilde{r} = [\tilde{r}_1^2 + \tilde{r}_2^2]^{1/2}$, $\tilde{r}_1 = \Gamma_r^{(1)}(s) - x_1$ and $\tilde{r}_2 = \Gamma_r^{(2)}(s) - x_2$. The second integrand function, \hat{P}_r^* , is presented in the following explicit form:

$$\hat{P}_r^*(\mathbf{x}, s) = -\frac{1}{4\pi(1-\nu)\tilde{r}} \begin{bmatrix} P_{11} & P_{12} \\ P_{21} & P_{22} \end{bmatrix}, \quad r = 1, 2, 3, \dots, n, \quad (7)$$

where

$$\begin{aligned}
 P_{11} &= \left\{ (1-2\nu) + 2\frac{\tilde{r}_1^2}{\tilde{r}^2} \right\} \frac{\partial \tilde{\mathbf{r}}}{\partial \mathbf{n}}, & P_{12} &= \left\{ 2\frac{\tilde{r}_1\tilde{r}_2}{\tilde{r}^2} \frac{\partial \tilde{\mathbf{r}}}{\partial \mathbf{n}} - (1-2\nu) \left[\frac{\tilde{r}_1}{\eta} n_2 + \frac{\tilde{r}_2}{\eta} n_1 \right] \right\}, \\
 P_{21} &= \left\{ 2\frac{\tilde{r}_2\tilde{r}_1}{\tilde{r}^2} \frac{\partial \tilde{\mathbf{r}}}{\partial \mathbf{n}} - (1-2\nu) \left[\frac{\tilde{r}_2}{\eta} n_1 + \frac{\tilde{r}_1}{\eta} n_2 \right] \right\}, & P_{22} &= \left\{ (1-2\nu) + 2\frac{\tilde{r}_2^2}{\tilde{r}^2} \right\} \frac{\partial \tilde{\mathbf{r}}}{\partial \mathbf{n}}, \\
 \frac{\partial \tilde{\mathbf{r}}}{\partial \mathbf{n}} &= \frac{\partial \tilde{r}_1}{\partial \tilde{\mathbf{r}}} n_1 + \frac{\partial \tilde{r}_2}{\partial \tilde{\mathbf{r}}} n_2.
 \end{aligned}$$

Having obtained a solution for the boundary with PIES (2), we can easily obtain a displacement value for any domain point by means of integral identity (5).

4. Stress in the domain

Knowing the distribution of displacements in the Ω_t domain, we can obtain the vector of strains as a result of proper differentiation of displacements. Then, using Hook's law, we can easily obtain stress distribution in the domain [14].

In our case, we can directly use integral identity (5) obtained for computing displacements in the domain. As a results of its proper differentiation and direct substitution into Hook's law, we have obtained the following integral expression for computing stress components in a polygonal domain:

$$\boldsymbol{\sigma}(\mathbf{x}) = \sum_{r=1}^n \int_{s_{r-1}}^{s_r} \left\{ \hat{\mathbf{D}}_r^*(\mathbf{x}, s) \mathbf{p}_r(s) - \hat{\mathbf{S}}_r^*(\mathbf{x}, s) \mathbf{u}_r(s) \right\} \mathbf{J}_r ds, \quad \boldsymbol{\sigma}(\mathbf{x}) = \{\sigma_x, \sigma_y, \tau_{xy}\}^T. \quad (8)$$

In this expression, integrands $\hat{\mathbf{D}}_r^*$ and $\hat{\mathbf{S}}_r^*$ are given in the following matrix form:

$$\hat{\mathbf{D}}_r^*(\mathbf{x}, s) = \frac{1}{4\pi(1-\nu)\tilde{\mathbf{r}}} \begin{bmatrix} (1-2\nu)\frac{\tilde{r}_1}{\tilde{\mathbf{r}}} + 2\frac{\tilde{r}_1^3}{\tilde{\mathbf{r}}^3} & -(1-2\nu)\frac{\tilde{r}_2}{\tilde{\mathbf{r}}} + 2\frac{\tilde{r}_2^2\tilde{r}_2}{\tilde{\mathbf{r}}^3} \\ (1-2\nu)\frac{\tilde{r}_2}{\tilde{\mathbf{r}}} + 2\frac{\tilde{r}_2^2\tilde{r}_2}{\tilde{\mathbf{r}}^3} & (1-2\nu)\frac{\tilde{r}_1}{\tilde{\mathbf{r}}} + 2\frac{\tilde{r}_1\tilde{r}_2^2}{\tilde{\mathbf{r}}^3} \\ -(1-2\nu)\frac{\tilde{r}_1}{\tilde{\mathbf{r}}} + 2\frac{\tilde{r}_1\tilde{r}_2^2}{\tilde{\mathbf{r}}^3} & (1-2\nu)\frac{\tilde{r}_2}{\tilde{\mathbf{r}}} + 2\frac{\tilde{r}_2^3}{\tilde{\mathbf{r}}^3} \end{bmatrix}, \quad (9)$$

$$\hat{\mathbf{S}}_r^*(\mathbf{x}, s) = \frac{\mu}{2\pi(1-\nu)\tilde{\mathbf{r}}^2} \begin{bmatrix} S_{11} & S_{12} \\ S_{21} & S_{22} \\ S_{31} & S_{32} \end{bmatrix}, \quad (10)$$

where

$$\begin{aligned}
 S_{11} &= 2\frac{\partial \tilde{\mathbf{r}}}{\partial \mathbf{n}} \left[(1-2\nu)\frac{\tilde{r}_1}{\tilde{\mathbf{r}}} + 2\nu\frac{\tilde{r}_1}{\tilde{\mathbf{r}}} - 4\frac{\tilde{r}_1^3}{\tilde{\mathbf{r}}^3} \right] + 4\nu n_1 \frac{\tilde{r}_1^2}{\tilde{\mathbf{r}}^2} + (1-2\nu) \left[2n_1 \frac{\tilde{r}_1^2}{\tilde{\mathbf{r}}^2} + 2n_1 \right] - (1-4\nu)n_1, \\
 S_{12} &= 2\frac{\partial \tilde{\mathbf{r}}}{\partial \mathbf{n}} \left[(1-2\nu)\frac{\tilde{r}_2}{\tilde{\mathbf{r}}} - 4\frac{\tilde{r}_1^2\tilde{r}_2}{\tilde{\mathbf{r}}^3} \right] + 4\nu n_1 \frac{\tilde{r}_1\tilde{r}_2}{\tilde{\mathbf{r}}^2} + (1-2\nu) \left[2n_2 \frac{\tilde{r}_1^2}{\tilde{\mathbf{r}}^2} \right] - (1-4\nu)n_2, \\
 S_{21} &= 2\frac{\partial \tilde{\mathbf{r}}}{\partial \mathbf{n}} \left[\nu\frac{\tilde{r}_2}{\tilde{\mathbf{r}}} - 4\frac{\tilde{r}_1^2\tilde{r}_2}{\tilde{\mathbf{r}}^3} \right] + 2\nu \left[n_1 \frac{\tilde{r}_1\tilde{r}_2}{\tilde{\mathbf{r}}^2} + n_2 \frac{\tilde{r}_1^2}{\tilde{\mathbf{r}}^2} \right] + (1-2\nu) \left[2n_1 \frac{\tilde{r}_1\tilde{r}_2}{\tilde{\mathbf{r}}^2} + n_2 \right], \\
 S_{22} &= 2\frac{\partial \tilde{\mathbf{r}}}{\partial \mathbf{n}} \left[\nu\frac{\tilde{r}_1}{\tilde{\mathbf{r}}} - 4\frac{\tilde{r}_1\tilde{r}_2^2}{\tilde{\mathbf{r}}^3} \right] + 2\nu \left[n_1 \frac{\tilde{r}_2^2}{\tilde{\mathbf{r}}^2} + n_2 \frac{\tilde{r}_1\tilde{r}_2}{\tilde{\mathbf{r}}^2} \right] + (1-2\nu) \left[2n_2 \frac{\tilde{r}_1\tilde{r}_2}{\tilde{\mathbf{r}}^2} + n_1 \right], \\
 S_{31} &= 2\frac{\partial \tilde{\mathbf{r}}}{\partial \mathbf{n}} \left[(1-2\nu)\frac{\tilde{r}_1}{\tilde{\mathbf{r}}} - 4\frac{\tilde{r}_1\tilde{r}_2^2}{\tilde{\mathbf{r}}^3} \right] + 4\nu n_2 \frac{\tilde{r}_1\tilde{r}_2}{\tilde{\mathbf{r}}^2} + (1-2\nu) \left[2n_1 \frac{\tilde{r}_2^2}{\tilde{\mathbf{r}}^2} \right] - (1-4\nu)n_1,
 \end{aligned}$$

$$S_{32} = 2 \frac{\partial \ddot{\vec{r}}}{\partial \mathbf{n}} \left[(1-2\nu) \frac{\vec{r}_2}{\vec{r}} + 2\nu \frac{\vec{r}_2}{\vec{r}} - 4 \frac{\vec{r}_2^3}{\vec{r}^3} \right] + 4\nu n_2 \frac{\vec{r}_2^2}{\vec{r}^2} + (1-2\nu) \left[2n_2 \frac{\vec{r}_2^2}{\vec{r}^2} + 2n_2 \right] - (1-4\nu)n_2,$$

$$\vec{r} = [\vec{r}_1^2 + \vec{r}_2^2]^{1/2}, \quad \vec{r}_1 = \Gamma_r^{(1)}(s) - x_1 \text{ and } \vec{r}_2 = \Gamma_r^{(2)}(s) - x_2.$$

5. Numerical solution of PIES

The PIES presented in Subsection 2.1 is characterized by containing an analytically defined boundary geometry. A practical definition of the polygonal boundary geometry is reduced to posing coordinates for the corner points. We can thus assume that the boundary geometry has been simply included in the PIES. The next step is an approximation of the boundary functions, which, in this case, means solving the obtained PIES. Therefore, the PIES's solution is no longer directly related to the boundary geometry, as the PIES is defined on a straight line in the parametrical system of reference.

The separation of the approximation of boundary geometry from that of boundary functions facilitates the latter and renders it more effective. Generally, the separation enables applying the numerical methods traditionally used to solve differential and integral equations and searching for even more effective methods suited to different types of boundary problems to be solved.

In earlier papers [9, 12, 15], a collocation method was used to solve the PIES obtained for Laplace and Helmholtz equations. As the method turned out to be simple and quite effective in a number of tested cases, it was selected for solving the PIES obtained for the Navier-Lamé equation. The method consists in approximating boundary functions $\mathbf{u}_r(s)$, $\mathbf{p}_r(s)$ on each segment r as follows:

$$\mathbf{p}_r(s) = \sum_{k=0}^N \mathbf{p}_r^{(k)} T_r^{(k)}(s), \quad \mathbf{u}_r(s) = \sum_{k=0}^N \mathbf{u}_r^{(k)} T_r^{(k)}(s), \quad (11)$$

where $\mathbf{u}_r^{(k)}$, $\mathbf{p}_r^{(k)}$ are unknown coefficients, N is the number of coefficients on segment r , and $T_r^k(s)$ are the global base functions on individual segments (Chebyshev polynomials).

The unknown coefficients for one of approximation series (11) on each segment are obtained as a result of interpolation of the posed boundary conditions. Coefficients of the other series are obtained after solving the PIES. Having substituted (11) into Equation (2), we obtain an expression for any given boundary conditions in the following general form:

$$\frac{1}{2} \mathbf{u}_p(s_1) = \sum_{r=1}^n \sum_{k=0}^N \left\{ \mathbf{p}_r^{(k)} \int_{s_{r-1}}^{s_r} \bar{\mathbf{U}}_{pr}^*(s_1, s) - \mathbf{u}_r^{(k)} \int_{s_{r-1}}^{s_r} \bar{\mathbf{P}}_{pr}^*(s_1, s) \right\} T_r^{(k)}(s) \mathbf{J}_r ds. \quad (12)$$

Having fulfilled the equation at collocation points $s_1 = s_{1(r)}$ ($r = 1, 2, 3, \dots, M$), $M = n \times N$ (total number of collocation points M being a product of the number of segments, n , and the number of unknown coefficients, N , on individual segments), we obtain an algebraic equation system with respect to unknown coefficients $\mathbf{p}_j^{(k)}$ or $\mathbf{u}_j^{(k)}$. On solving this equation, we obtain the unknown coefficients from one of approximation series (11). When these are substituted into Equation (11), an

analytical expression for an unknown boundary function is obtained, from which we can obtain a solution at any given point for any boundary segment.

The accuracy of the results obtained by this method is largely dependent on N and, to a lesser degree, on the arrangement of collocation points and the complexity of the posed boundary conditions. In accordance with earlier research for the Laplace equation, the most accurate results were obtained when extreme collocation points were placed close to the segments' ends. Highly accurate solutions were obtained even for an algebraic equation system much smaller than in the traditional BEM [12].

The proposed technique is quite simple from the programmatic point of view and highly effective in practical applications. It enables optimal arrangement of collocation points and choosing an exact number of expressions, N , in approximation series (11), depending on the length of segments r . This is a very significant advantage, as segments r may have diverse lengths when corner points are used in modeling the boundary geometry with a PIES. In order to obtain accurate results on each segment, it is necessary merely to choose an N dependent on the length of segment r and the complexity of the posed boundary conditions.

The proposed method of approximating boundary functions is especially effective from the point of view of analysis of the solutions' convergence. In order to perform it, We only need to change number N from series (11), which stands for the number of accepted expressions. The process is technically much easier than another discretization of the domain or the boundary into smaller elements.

Having found the functions on the boundary, we can obtain the solution in domain Ω on the basis of integral identity (5).

Finally, Equation (12) written for all the collocation points [9, 12] assumes the form of an algebraic equation system approximating the PIES:

$$Hu = Gp. \tag{13}$$

In the above system, \mathbf{u} or \mathbf{p} are unknown coefficients. Which of the functions in Equation (11) is known and which is to be found will depend on the type of the boundary problem to be solved. Having solved Equation (13), we obtain unknown coefficients \mathbf{u} or \mathbf{p} , which – after substitution to Equation (11) – yield a solution on the boundary Γ_t for a homogeneous domain Ω_t .

One of the PIES's advantages is that solutions obtained on the boundary with expressions (11) are continuous (in contrast to BEM). It enables obtaining a solution for any boundary point by substitution of parameter s (which corresponds to the point's coordinates in the Cartesian reference system) into Equation (11).

5.1. Numerical solution in the domain

Boundary functions $\mathbf{p}_r(s)$, $\mathbf{u}_r(s)$ from Equation (5) are necessary to obtain solutions in the domain. One of them is given in the form of boundary conditions, whilst the other is obtained after solving the PIES. Assuming that both functions are approximated by approximation series (11) and substituting them into Equation (5), we obtain:

$$\mathbf{u}(\mathbf{x}) = \sum_{r=1}^n \sum_{k=0}^N \left\{ \mathbf{p}_r^{(k)} \int_{s_{r-1}}^{s_r} \bar{U}_{pr}^*(s_1, s) - \mathbf{u}_r^{(k)} \int_{s_{r-1}}^{s_r} \bar{P}_{pr}^*(s_1, s) \right\} T_r^{(k)}(s) \mathbf{J}_r ds. \tag{14}$$

It follows from Equation (14) that only coefficients $\mathbf{p}_r^{(k)}$, $\mathbf{u}_r^{(k)}$ from approximation series (11) are required for practical solution of domain Ω_t at any point. The first vector of coefficients is obtained after solving the PIES, the second – after approximation of the given boundary condition.

6. A PIES for a domain built with subregions of different material constants

It is also possible to obtain a PIES for domain Ω composed of subregions Ω_t of different material constants. The problem is to obtain a fundamental and singular boundary solution in an explicit form. The solution should take into account linear segments limiting subregions and the material constants of each subregion Ω_t .

The considered problem could be easier to solve if we treated the polygonal domain Ω as a sum of subregions Ω_t , $t = 1, 2, \dots, m$. A geometrical interpretation of a boundary with three polygonal subregions is shown in Figure 2. Only 4 corner points and 4 external points on the common interfaces are required to define such boundary geometry (regardless of the domain's area).

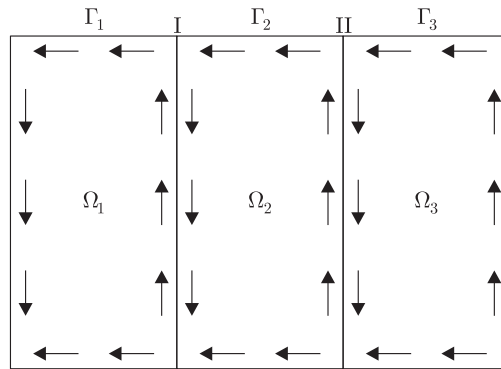


Figure 2. Domain Ω with three subregions Ω_t ($t = 1, 2, 3$)

As each subregion Ω_t ($t = 1, 2, 3$, see Figure 2), is characterized by different material constants E_t , ν_t , it is necessary to apply the PIES to each subregion individually. Thereafter, we can connect the subregions on common interfaces I and II by means of compatibility conditions. Finally, the following integral equation system is obtained:

$$\frac{1}{2} \mathbf{u}_p(s_1) = \sum_{r=1}^n \mathbf{J}_r \int_{s_{r-1}}^{s_r} \{ \bar{\mathbf{U}}_{pr}^*(s_1, s) \mathbf{p}_r(s) - \bar{\mathbf{P}}_{pr}^*(s_1, s) \mathbf{u}_r(s) \} ds \quad \text{for } \Omega_1, \quad (15)$$

$$\mathbf{u}_1^I(s) = \mathbf{u}_2^I(s) = \mathbf{u}^I(s), \quad \mathbf{p}_1^I(s) = -\mathbf{p}_2^I(s) = \mathbf{p}^I(s) \quad \text{for } \Gamma_1, \quad (16)$$

$$\frac{1}{2} \mathbf{u}_p(s_1) = \sum_{r=1}^n \mathbf{J}_r \int_{s_{r-1}}^{s_r} \{ \bar{\mathbf{U}}_{pr}^*(s_1, s) \mathbf{p}_r(s) - \bar{\mathbf{P}}_{pr}^*(s_1, s) \mathbf{u}_r(s) \} ds \quad \text{for } \Omega_2, \quad (17)$$

$$\mathbf{u}_2^{II}(s) = \mathbf{u}_3^{II}(s) = \mathbf{u}^{II}(s), \quad \mathbf{p}_2^{II}(s) = -\mathbf{p}_3^{II}(s) = \mathbf{p}^{II}(s) \quad \text{for } \Gamma_2, \quad (18)$$

$$\frac{1}{2} \mathbf{u}_p(s_1) = \sum_{r=1}^n \mathbf{J}_r \int_{s_{r-1}}^{s_r} \{ \bar{\mathbf{U}}_{pr}^*(s_1, s) \mathbf{p}_r(s) - \bar{\mathbf{P}}_{pr}^*(s_1, s) \mathbf{u}_r(s) \} ds \quad \text{for } \Omega_3. \quad (19)$$

Having applied algebraic approximation individually to Equations (15), (17) and (19), we obtain:

$$[\mathbf{H}_1 \quad \mathbf{H}_1^I] \begin{bmatrix} \mathbf{u}_1 \\ \mathbf{u}_1^I \end{bmatrix} = [\mathbf{G}_1 \quad \mathbf{G}_1^I] \begin{bmatrix} \mathbf{p}_1 \\ \mathbf{p}_1^I \end{bmatrix} \quad \text{for subregion } \Omega_1, \quad (20)$$

$$[\mathbf{H}_2 \quad \mathbf{H}_2^I] \begin{bmatrix} \mathbf{u}_2 \\ \mathbf{u}_2^I \end{bmatrix} = [\mathbf{G}_2 \quad \mathbf{G}_2^I] \begin{bmatrix} \mathbf{p}_2 \\ \mathbf{p}_2^I \end{bmatrix} \quad \text{for subregion } \Omega_2, \text{ and} \quad (21)$$

$$[\mathbf{H}_3 \quad \mathbf{H}_3^{II}] \begin{bmatrix} \mathbf{u}_3 \\ \mathbf{u}_3^{II} \end{bmatrix} = [\mathbf{G}_3 \quad \mathbf{G}_3^{II}] \begin{bmatrix} \mathbf{p}_3 \\ \mathbf{p}_3^{II} \end{bmatrix} \quad \text{for subregion } \Omega_3. \quad (22)$$

As a result of connecting Equations (20), (21) and (22) with compatibility condition (16), (18), the following approximate system of algebraic equations is obtained for the three subregions:

$$\begin{bmatrix} \mathbf{H}_1 & \mathbf{H}_1^I & -\mathbf{G}_1^I & 0 & 0 \\ 0 & \mathbf{H}_2^I & -\mathbf{G}_2^I & \mathbf{H}_2 & 0 \\ 0 & 0 & \mathbf{H}_3^{II} & -\mathbf{G}_3^{II} & \mathbf{H}_3 \end{bmatrix} \begin{bmatrix} \mathbf{u}_1 \\ \mathbf{u}_1^I \\ \mathbf{p}_1^I \\ \mathbf{u}_3^{II} \\ \mathbf{u}_3 \end{bmatrix} = \begin{bmatrix} \mathbf{G}_1 & 0 & 0 \\ 0 & \mathbf{G}_2 & 0 \\ 0 & 0 & \mathbf{G}_3 \end{bmatrix} \begin{bmatrix} \mathbf{p}_1 \\ \mathbf{p}_2 \\ \mathbf{p}_3 \end{bmatrix}. \quad (23)$$

Considering the boundary condition, Equation (23) assumes the following form:

$$\mathbf{A}\mathbf{X} = \mathbf{B}, \quad (24)$$

where \mathbf{X} is a vector of the unknown coefficients of approximation series (11).

Vector \mathbf{X} is dependent on unknown coefficients \mathbf{u} or \mathbf{p} approximating boundary functions (11). If we have displacements as given, \mathbf{p} is the unknown function to be found; when surface forces are given – the unknown function is \mathbf{u} . In a mixed problem, vector \mathbf{X} contains coefficients \mathbf{p} and \mathbf{u} alternate with given coefficients \mathbf{u} and \mathbf{p} on each of the segments. In all boundary problems, both coefficients are searched on interfaces between subregions.

\mathbf{A} is a blocked and banded matrix, of sample graphical presentation shown in Figure 3.

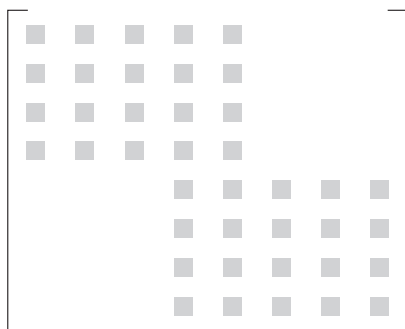


Figure 3. Matrix \mathbf{A} for two subregions

The Gauss elimination method [16] is applied to solve algebraic equation system (24).

7. Testing the proposed algorithm

As there are no analytical solutions for such problems, the proposed algorithm has been tested on reliable numerical solutions.

First, we solved a problem defined in a region Ω by means of a pre-tested program based on the PIES. Its had been tested on numerous examples with analytical solutions [13].

Thereafter, the proposed algorithm was tested on the same examples assuming that domain Ω was composed of two subregions, Ω_1 and Ω_2 , of the same material constants. While the condition did not change the problem from the point of view of material constants in the whole domain, it enabled testing the proposed algorithm on connected subregions as for the Laplace equation [17]. The main purpose of the following examples is to compare solutions obtained from two different programs. We will first solve the problem with a program for a single region and then with the proposed program for subregions.

7.1. Example 1

In our first example we consider a square domain with boundary conditions as per Figure 4.

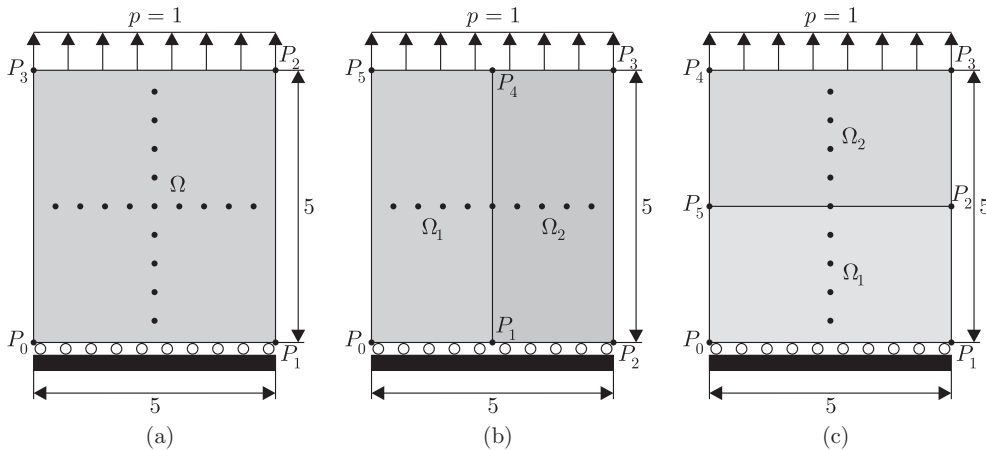


Figure 4. Boundary conditions, boundary geometry and domain division for Example 1

We assume the domain to consist of two polygonal subregions with the same material constants $E_1 = E_2 = 1$, $\nu_1 = \nu_2 = 0.25$. The algorithm presented in the paper (for two subregions) is applied to solve problem, but we also use the previously obtained program for a single region.

When applying the PIES to two subregions (see Figure 4b), it is necessary to set six corner points P_i ($i = 0, 1, \dots, 5$), whilst four corner points, P_0, P_1, P_2, P_3 , need to be posed when using the PIES for a single region (see Figure 4a). Solutions at selected points of the subregions are compared with those obtained for a single region in Table 1. The numerical results obtained for a single region (columns 2 and 3) are close to the results for two subregions presented in columns 4 and 5. Minor differences are due to the fact that in the case of connected subregions the number of expressions

Table 1. Solutions obtained for cross-section $x = 2.5$ and $0 < y < 5$ (see Figure 4b)

Coordinates of points	Single region $E = 1, \nu = 0.25$		Two subregions			
			$E_1 = E_2 = 1$ $\nu_1 = \nu_2 = 0.25$		$E_1 = 2, E_2 = 1$ $\nu_1 = 0.25, \nu_2 = 0.3$	
	u_1	u_2	u_1	u_2	u_1	u_2
1	2	3	4	5	6	7
(2.5, 0.5)	$-7.0157 \cdot 10^{-7}$	0.46629	$1.8692 \cdot 10^{-13}$	0.46933	$3.0547 \cdot 10^{-13}$	0.46481
(2.5, 1)	$-3.6669 \cdot 10^{-6}$	0.93338	$4.1362 \cdot 10^{-13}$	0.94604	$6.8144 \cdot 10^{-13}$	0.94427
(2.5, 1.5)	$-6.4391 \cdot 10^{-6}$	1.41933	$6.7425 \cdot 10^{-13}$	1.44074	$1.1182 \cdot 10^{-12}$	1.44310
(2.5, 2)	$-8.8518 \cdot 10^{-6}$	1.91744	$9.5927 \cdot 10^{-13}$	1.94582	$1.6013 \cdot 10^{-12}$	1.95011
(2.5, 2.5)	$-1.0895 \cdot 10^{-5}$	2.42167	0.00630962	2.43049	0.00197652	2.44962
(2.5, 3)	$-1.2664 \cdot 10^{-5}$	2.92777	$1.5106 \cdot 10^{-12}$	2.95736	$2.4525 \cdot 10^{-12}$	2.70850
(2.5, 3.5)	$-1.4303 \cdot 10^{-5}$	3.43326	$1.7434 \cdot 10^{-12}$	3.46888	$2.7675 \cdot 10^{-12}$	2.96758
(2.5, 4)	$-1.5916 \cdot 10^{-5}$	3.93721	$1.9757 \cdot 10^{-12}$	3.97545	$3.0796 \cdot 10^{-12}$	3.22237
(2.5, 4.5)	$-1.7479 \cdot 10^{-5}$	4.43985	$2.2147 \cdot 10^{-12}$	4.47832	$3.3942 \cdot 10^{-12}$	3.47515

Table 2. Solutions obtained for cross-section $y = 2.5$ and $0 < x < 5$ (see Figure 4c)

Coordinates of points	Single region $E = 1, \nu = 0.25$		Two subregions			
			$E_1 = E_2 = 1$ $\nu_1 = \nu_2 = 0.25$		$E_1 = 2, E_2 = 1$ $\nu_1 = 0.25, \nu_2 = 0.3$	
	u_1	u_2	u_1	u_2	u_1	u_2
1	2	3	4	5	6	7
(0.5, 2.5)	0.49233	2.48751	0.49648	2.49081	0.61345	2.50320
(1, 2.5)	0.36655	2.46003	0.36745	2.45844	0.57208	2.31712
(1.5, 2.5)	0.24215	2.43876	0.24230	2.43419	0.53035	2.12944
(2, 2.5)	0.12021	2.42591	0.12036	2.41937	0.49152	1.94260
(2.5, 2.5)	$-1.089 \cdot 10^{-5}$	2.42167	$-2.374 \cdot 10^{-5}$	2.41561	0.41474	1.77206
(3, 2.5)	-0.12023	2.42591	-0.12041	2.41938	0.38185	1.59651
(3.5, 2.5)	-0.24217	2.43876	-0.24235	2.43420	0.31580	1.44074
(4, 2.5)	-0.36657	2.46004	-0.36750	2.45846	0.24921	1.29454
(4.5, 2.5)	-0.49235	2.48752	-0.49654	2.49083	0.18014	1.15415

in approximation series (11) should be increased in order to obtain more accurate results.

Considering care taken in testing the program for a single region, we can assume the algorithm for two subregions to be equally reliable and suitable for solving problems with different material constants. Solutions for different material constants are presented in columns 6 and 7 of Table 1.

Table 2 contains solutions obtained in the domain divided as per Figure 4c. Comparing the values presented in columns 2 and 4 with those of 3 and 5, the solutions are noticeable more accurate those shown in Table 1.

Table 3. Solutions obtained for cross-section $y = 1$ and $0 < x < 4$ (see Figure 5)

Coordinates of points	Single region $E = 26, \nu = 0.3$		Two subregions			
			$E_1 = E_2 = 26$ $\nu_1 = \nu_2 = 0.3$		$E_1 = 26, E_2 = 30$ $\nu_1 = 0.2, \nu_2 = 0.3$	
	u_1	u_2	u_1	u_2	u_1	u_2
(0.4,1.0)	-0.18767	-0.34675	-0.18112	-0.34547	-0.11402	-0.37778
(0.8,1.0)	-0.13173	-0.32103	-0.12450	-0.31736	-0.08034	-0.35232
(1.2,1.0)	-0.08293	-0.30519	-0.07493	-0.29838	-0.05082	-0.33173
(1.6,1.0)	-0.03960	-0.29527	-0.03131	-0.28470	-0.02519	-0.31205
(2.0,1.0)	0.00094	-0.29105	0.00817	-0.27722	-0.00421	-0.29212
(2.4,1.0)	0.04116	-0.29359	0.04774	-0.28282	0.03480	-0.27277
(2.8,1.0)	0.08366	-0.30298	0.08812	-0.29587	0.07237	-0.26855
(3.2,1.0)	0.13147	-0.31992	0.13508	-0.31583	0.11269	-0.27615
(3.6,1.0)	0.18658	-0.34771	0.19002	-0.34634	0.15920	-0.29553

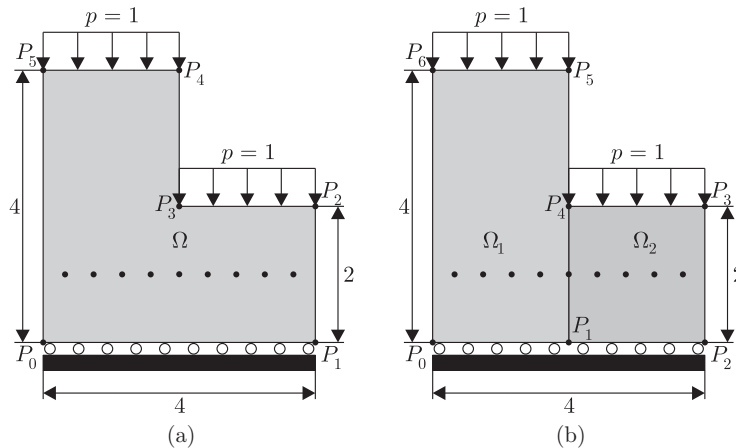


Figure 5. Boundary conditions and defining boundary geometry with corner points in Example 2

7.2. Example 2

In order to test the proposed method even more accurately on a more complicated boundary geometry, we shall now consider the problem presented in Figure 5.

Only seven corner points P_i ($i = 0, 1, \dots, 6$) are required to define the problem's boundary geometry. We can also solve the problem with the PIES for a single region [13], for which only six corner points, $P_0, P_1, P_2, P_3, P_4, P_5$, are required. Solutions for the selected points of subregions, as shown in Figure 5, are presented in Table 3 for both solution methods. The obtained results confirm reliability of the proposed method for different boundary conditions and greater numbers of subregions.

7.3. Example 3

In our last example, a rectangular domain is considered with two sides much longer than the others. An example of such domain is a beam. Dimensions of the

Table 4. Solutions obtained on the upper horizontal boundary (see Figure 6)

Coordinates of points	Single region $E = 1, \nu = 0.1$	Two subregions	
		$E_1 = E_2 = 1$ $\nu_1 = \nu_2 = 0.1$	$E_1 = 1, E_2 = 2$ $\nu_1 = \nu_2 = 0.1$
		u_1	
(0,1)	$-2.63 \cdot 10^{-6}$	$-2.51 \cdot 10^{-6}$	0.0008
(1,1)	1.1842	1.1842	1.0163
(2,1)	2.3684	2.3684	2.0266
(3,1)	3.5526	3.5526	3.0132
(4,1)	4.7368	4.7368	3.9663
(5,1)	5.9210	5.9210	4.5075
(6,1)	7.1052	7.1052	5.0585
(7,1)	8.2894	8.2894	5.6262
(8,1)	9.4736	9.4737	6.2055

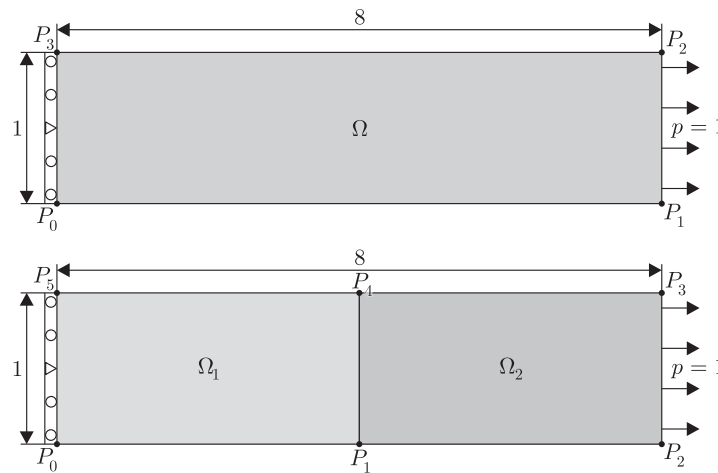


Figure 6. Boundary conditions, boundary geometry and domain division in Example 3

considered beam and the given boundary conditions are presented in Figure 6. The beam has been divided into two subregions of zonal material heterogeneity.

In order to test the proposed algorithm, solutions on boundary $P_2 P_3$ obtained for the whole domain and for the two subdomains with the same material constants were compared. The results are presented in Table 4.

Displacements u_1 obtained for the whole domain and its division into two subregions with the same material constants are almost equal. We can thus assume that the algorithm yields regular results with subregions and is capable of solving problems of subregions with different material constants. Exemplary solutions for such subregions are presented in the last column of Table 4.

8. Conclusions

We have presented a new non-element method for modeling boundary geometry in boundary problems described by the Navier-Lamé equation in which only corner

points of a polygonal domain are set. The number of such points is much less than the number of nodes used in FEM or BEM. An important advantage of the proposed approach is that the number of points is independent of the domain's area. Therefore, the effectiveness of such definition increases with increasing domain area.

Application of the proposed boundary geometry definition is only possible in a previously obtained PIES, an analytical modification of the traditional BIE. The achieved effectiveness in solving of unconnected domains encourages the method's generalization onto connected regions with different material constants.

Our test examples have confirmed the proposed algorithm's effectiveness in the case of connected regions.

Acknowledgements

The present research work was financed from the Polish science budget for years 2005–2007 – project number 3T11F01528.

References

- [1] Zienkiewicz O 1977 *The Finite Element Method*, McGraw-Hill, London
- [2] Brebbia C A, Telles J C F and Wrobel L C 1984 *Boundary Element Techniques, Theory and Applications in Engineering*, Springer-Verlag, New York
- [3] Wu Ch, Lin Ch and Chiou Y 1996 *Computers and Geotechnics* **19** (2) 75
- [4] Perez-Gavilan J J and Aliabadi M H 2001 *Engineering Analysis with Boundary Elements* **25** 633
- [5] Lu X and Wu W 2005 *Engineering Analysis with Boundary Elements* **29** 944
- [6] Atalay M A, Aydin E D and Aydin M 2004 *Int. J. Heat and Mass Transfer* **47** 1549
- [7] Foley J D 1993 *Computer Graphics: Principles and Practice*, Addison-Wesley, Massachusetts
- [8] Zieniuk E 2003 *Engineering Analysis with Boundary Elements* **26** (10) 897
- [9] Zieniuk E 2003 *Int. J. Solids and Structures* **40** (9) 2301
- [10] Zieniuk E 2003 *Engng Comput.* **20** (2) 112
- [11] Gottlieb D and Orszag S A 1977 *Numerical Analysis of Spectral Methods*, SIAM, Philadelphia
- [12] Zieniuk E 2001 *Engineering Analysis with Boundary Elements* **25** (3) 185
- [13] Zieniuk E and Bołtuć A 2006 *Int. J. Solids and Structures* **43** 7939
- [14] Fung Y C 1965 *Foundations of Solid Mechanics*, Prentice Hall
- [15] Zieniuk E and Bołtuć A 2006 *J. Comput. Acoustics* **14** (3) 353
- [16] Hoffman J D 2001 *Numerical Methods for Engineers and Scientists*, Marcel Dekker Inc., New York
- [17] Szczebiot R and Zieniuk E 2002 *Proc. 15th Nordic Seminar on Computational Mechanics*, Poland, pp. 275–278